




Asteroids and Life: How Special Is the Solar System?

Rebecca G. Martin^{1,2}  and Mario Livio¹¹Department of Physics and Astronomy, University of Nevada, Las Vegas, 4505 South Maryland Parkway, Las Vegas, NV 89154, USA²Nevada Center for Astrophysics, University of Nevada, Las Vegas, NV 89154, USA

Received 2021 December 13; revised 2022 January 20; accepted 2022 February 2; published 2022 February 18

Abstract

Asteroid impacts with Earth may have played an essential role in the emergence of life on Earth through their creation of favorable niches for life, changes to the atmosphere, and delivery of water. Consequently, we suggest two potential requirements for life in an exoplanetary system: first, that the system has an asteroid belt, and second, that there is a mechanism to drive asteroids to impact the terrestrial habitable planet. Since in the solar system the ν_6 secular resonance has been shown to have been important in driving these impacts, we explore how the masses and locations of two giant planets determine the location and strength of this secular resonance. Examining observed exoplanetary systems with two giant planets, we find that a secular resonance within the asteroid belt region may not be uncommon. Hence, the solar system is somewhat special, but the degree of fine-tuning that may be necessary for the emergence of life is not excessive. Finally, with n -body simulations, we show that when the two giant planets are close to the 2:1 mean motion resonance, the asteroid belt is unstable, but this does not lead to increased asteroid delivery.

Unified Astronomy Thesaurus concepts: [Asteroid belt \(70\)](#); [Asteroid dynamics \(2210\)](#); [Habitable planets \(695\)](#)

1. Introduction

Studies of the origin of life on Earth have made impressive progress in the past decade (see, e.g., Sutherland 2016, 2017; Szostak 2017a, 2017b, for recent reviews). While many questions remain open, there is a growing consensus on many aspects of the processes involved. For example, it appears that hydrogen cyanide, which today is considered a deadly poison, may have provided the primordial pathway from prebiotic chemistry to life. In this work we are interested specifically in the role that asteroid impacts may have played in the emergence of life on Earth. Unfortunately, one of the effects of plate tectonics has been to erase most of the traces of the early geological evolution of Earth's surface. However, most researchers agree that Earth experienced a relatively high impact rate during roughly the first billion years of its existence (e.g., Bottke & Norman 2017).

For a few decades, the dominant opinion has been that asteroid impacts have impeded rather than aided the emergence of life on Earth (see, e.g., discussion by Sleep 2018). More recently, however, opinions started to swing in the other direction, suggesting that asteroid impacts may have, in fact, been essential for the transition from chemistry to biology (see, e.g., Osinski et al. 2020, for an extensive review and references therein). According to the new scenario, impacts may have acted both as generators of favorable niches for life to emerge (niches such as impact crater lakes and shocked rocks) and as the agents that had changed the entire Earth environment in a way that made it conducive for life (e.g., by producing atmospheric hydrogen cyanide). Asteroid impacts may have delivered water to the surface of Earth (Morbidelli et al. 2000; Martin & Livio 2021) and led to the formation of the Moon (e.g., Canup 2012; Ćuk & Stewart 2012).

Another crucial effect for the origin of life could have been created by relatively large impacts during the “late veneer” (material accreted by Earth after the formation of the Moon). Such impacts could have produced a reduced atmosphere of the early Earth, when the iron core of the impactor reacted with water in the oceans. As the iron oxidized, the hydrogen was released, resulting in an atmosphere (which could have lasted a few million years) favoring the emergence of simple organic molecules (e.g., Zahnle et al. 2020; see also Genda et al. 2017a, 2017b; Benner et al. 2020).

Given the mounting evidence for the potential role of asteroids in the emergence of life on Earth, it is not unreasonable to *assume* that asteroid impacts on a terrestrial planet (in the habitable zone of its host star) are a necessary condition for the emergence of life and to study the consequences of this assumption. This hypothesis dictates two requirements for an exoplanetary system to harbor life:

1. The system has to contain the equivalent of an asteroid belt.
2. The system has to have a mechanism that drives asteroids out of the belt and causes them to impact the terrestrial planet.

In the present work we explore under which conditions planetary systems can satisfy these two requirements, as well as the implications of these conditions for the important question of whether the solar system is in any way special, when compared to other confirmed exoplanetary systems. In Section 2 we examine the formation of asteroid belts. In Section 3 we explore the location and strength of secular resonances with different giant planetary system architectures and compare to observed exoplanetary systems. In Section 4 we run simulations to test the efficiency of asteroid impacts from the belt. A discussion and conclusions follow in Section 5.



Original content from this work may be used under the terms of the [Creative Commons Attribution 4.0 licence](#). Any further distribution of this work must maintain attribution to the author(s) and the title of the work, journal citation and DOI.

2. The Formation of Asteroid Belts

The snow line radius is the distance from the central star outside of which water is found in the form of ice. It occurs at a temperature of around $T_{\text{snow}} = 170$ K in the protoplanetary disk (Hayashi 1981; Lecar et al. 2006). The snow line radius evolved with the protoplanetary gas disk, likely beginning farther out and moving inward as the disk temperature cooled (Garaud & Lin 2007; Martin & Livio 2013b). In our solar system today, the composition of the asteroids in the belt has a transition at a radius of about 2.7 au (DeMeo & Carry 2014), suggesting that the snow line radius may have been located there in the asteroid belt at the time at which the gas disk dissipated (Abe et al. 2000; Morbidelli et al. 2010). Recent studies have shown that the compositional gradient may be explained by the gas giant’s growth and/or migration (e.g., Raymond & Izidoro 2017a).

In protoplanetary disks, the solid mass density increases significantly outside of the snow line (Pollack et al. 1996). Consequently, giant planets likely form outside of the snow line radius (Kennedy & Kenyon 2008), and asteroid belts likely form around the location of the water snow line radius, inside of the giant planets (Martin & Livio 2013a). Observations of debris disks show that it is common for there to be two components to the disk, similar to the asteroid belt and the Kuiper Belt in the solar system (Kennedy & Wyatt 2014; Geiler & Krivov 2017; Rebollido et al. 2018). The gap between the two belts is likely caused by planet formation. Ballering et al. (2017) found that the warm components in single-component systems follow the primordial snow line, so they likely arise from asteroid belts (see also Morales et al. 2011).

Observations of exoplanets initially suggested that Jupiter was somewhat of an outlier in terms of its orbital location (Beer et al. 2004; Martin & Livio 2015). However, more recent exoplanet detections with the radial velocity and microlensing methods have shown that the location of Jupiter is not particularly special. In fact, there is a peak in the occurrence of giant planets at around 2–3 au, close to the snow line radius (Fernandes et al. 2019; Nielsen et al. 2019). However, the frequency of planets with masses of 0.1–20 M_J (where M_J is the mass of Jupiter) between 0.1 and 100 au is only about 26%, and it drops to 6.2% if only planets more massive than Jupiter are included. Thus, Jupiter-like planets are somewhat rare (see also Wittenmyer et al. 2016). Note that giant exoplanets that are found close to their host stars have likely undergone some type of migration from where they formed.

In this work we consider the classical picture in which an asteroid belt forms because perturbations from an outer giant planet prevent material from forming a planet. Violent collisions lead to fragmentation rather than accretion (Wetherill & Stewart 1989).³ For a relatively small giant planet eccentricity, the outer edge of an asteroid belt likely occurs roughly at the location of the 2:1 mean motion resonance (MMR) with the giant planet. In the solar system this is at about $a_{\text{out}} = 3.3$ au = $0.63 a_J$, where a_J is the semimajor axis of Jupiter. The inner edge of the asteroid belt is not so well defined. It should be at the radius at which the perturbations from the giant planet become small enough that planet formation can proceed. Based on the solar system, in this

work we take the inner edge to be close to the orbit of Mars, $a_{\text{in}} = 1.5$ au = $0.29 a_J$. We also assume that the radial extent of an asteroid belt scales simply with the location of the innermost giant planet.

3. The ν_6 Secular Resonance

Most solar system models to date have focused on the idea that the giant planets cleared out material from the asteroid region (Chambers & Wetherill 2001; Petit et al. 2001; O’Brien et al. 2007; Nesvorný et al. 2021).⁴ While MMRs may play a role in asteroid delivery, in the solar system, the ν_6 resonance is the strongest resonance in the asteroid belt (e.g., Froeschle & Scholl 1986; Morbidelli & Henrard 1991). The resonance occurs where the precession rate of a test particle is equal to the eigenfrequency of Saturn. It causes asteroids in the region to become eccentric and collide with Earth with a relatively high probability of a few percent (Ito & Malhotra 2006; Haghighipour & Winter 2016; Martin & Livio 2021). Without the ν_6 resonance in the asteroid belt, the number of asteroid collisions with Earth is significantly reduced (Morbidelli et al. 1994; Bottke et al. 2000; Smallwood et al. 2018a).

3.1. Location of the ν_6 Resonance

We examine the location of the ν_6 resonance for varying giant planet architectures with a linear theory (Dermott & Nicholson 1986; Murray & Dermott 2000), including a correction due to the 2:1 MMR between the planets (Malhotra et al. 1989; Minton & Malhotra 2011). The giant planets were taken to have masses of m_1 and m_2 and orbits with semimajor axes a_1 and a_2 , respectively, around a host star of mass M_* . We vary the relative semimajor axis and mass of the outer giant planet. The eccentricities of the planets were assumed to be 0.05 unless otherwise stated.

Figure 1 shows the location of the ν_6 resonance for three different inner planet masses. The colored regions show where the resonance falls in the approximate range for an asteroid belt given by $0.29 < a_{\nu_6}/a_1 < 0.63$. The vertical dashed line shows the location of the 2:1 resonance between the two planets. The location of the ν_6 resonance does not change significantly with the mass ratio of the planets, but it is very sensitive to the semimajor axis ratio. Generally, the resonance moves outward with decreasing semimajor axis of the outer planet, until the planets approach the 2:1 MMR and there is no longer a ν_6 resonance within the belt. Note that had we chosen a larger inner radius for the belt, the colored region would be truncated on the right-hand side and the planets would need to be closer together in order for a resonance to exist in the belt.

We should note that a secular resonance could also be formed with a giant planet and an outer binary star companion. While the star is much more massive than a giant planet, it is also much farther away (see also Smallwood et al. 2018b), but in this work we focus on the effects of planetary systems.

3.2. Strength of the ν_6 Resonance

While the location of the resonance does not vary much with outer planet mass, the strength of the resonance does. Figure 2 shows the width of the secular resonance, w , which we define

³ Several new studies suggest that the belt in the solar system may have initially been empty and later populated by planetesimals scattered from other locations (Raymond & Izidoro 2017b; Raymond & Nesvorný 2020). In this scenario, a giant planet may not be a requirement for an asteroid belt to form.

⁴ Note that planetary embryos that are embedded in an asteroid belt may lead to perturbations and eccentricity excitation, although models all include Jupiter and Saturn at their current location and hence also involve resonances (e.g., O’Brien et al. 2007).

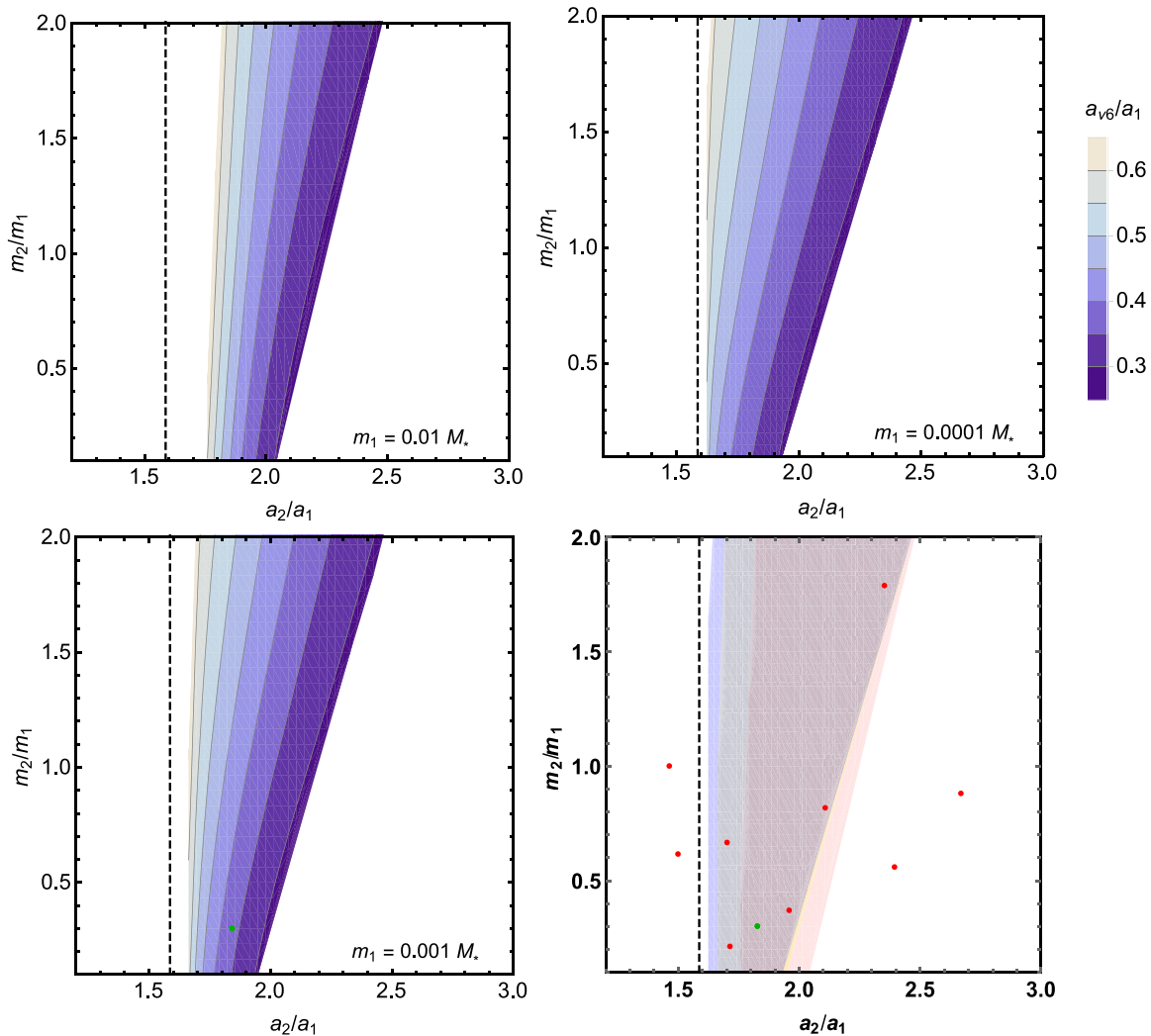


Figure 1. Location of the resonance as a fraction of the inner giant’s semimajor axis, a_{ν_6}/a_1 . The colored regions show where the resonance is in the radial range $0.29 < a_{\nu_6}/a_1 < 0.63$ for varying mass and semimajor axis of the outer giant planet scaled to those of the inner planet. The dashed vertical lines represent the 2:1 MMR between the two giants. The inner planet has a mass of $m_1 = 0.01 M_*$ (top left), $m_1 = 0.001 M_*$ (bottom left), and $m_1 = 0.0001 M_*$ (top right). The green points shows the solar system. Bottom right: relative mass and semimajor axis of exoplanet planet pairs shown in Table 1 (red points). The shaded regions show where the ν_6 resonance lies within the asteroid belt region for inner planet masses $m_1 = 0.0001 M_*$ (blue), $m_1 = 0.001 M_*$ (yellow), and $m_1 = 0.01 M_*$ (red).

to be the radial range where the forced eccentricity of a test particle is $e_f > 0.08$. We only show the width for parameters for which the resonance lies within the belt. Generally, the closer in and higher the mass of the outer planet (for fixed inner planet mass and semimajor axis), the wider the resonance and therefore the higher the number of asteroids that collide with the terrestrial planet. The eccentricities of the giant planets do not affect the location of the resonance, but they do affect the width. A higher eccentricity of the inner planet leads to an increase in the average eccentricity of the belt but does not significantly change the resonance. However, the outer planet eccentricity has a strong effect on the resonance. The bottom right panel of Figure 2 shows a higher-eccentricity outer planet. The resonance may be very wide and destroy the entire belt on a short timescale for a high-eccentricity outer planet. In this case there may be initially a very high rate of impacts but a much lower rate on long timescales.

3.3. The ν_6 Resonance in Exoplanetary Systems

Table 1 shows all of the multiplanet systems in the NASA Exoplanet Archive for which at least two planets have both their semimajor axis and mass determined. We have kept only planets that are at an orbital semimajor axis greater than 2 au and that have a mass greater than $0.1 M_J$. We removed the system TYC 8998-760-1 since its planets are at distances of hundreds of astronomical units. For systems that have more than two giant planets that satisfy our criteria, we considered the innermost two planets. For each planet pair we estimated the location and width of the ν_6 resonance. In the calculations we only included the two planets represented in the table. The red points in the bottom right panel of Figure 1 show the observed data. We also shaded three regions that show where the location of the ν_6 resonance falls within the asteroid belt region for different inner planet masses.

Due to the difficulty in detecting giant planets at large orbital radii, the observed systems are significantly affected by selection effects. However, out of the 13 systems (other than the solar system), we find that 4 have a configuration such that

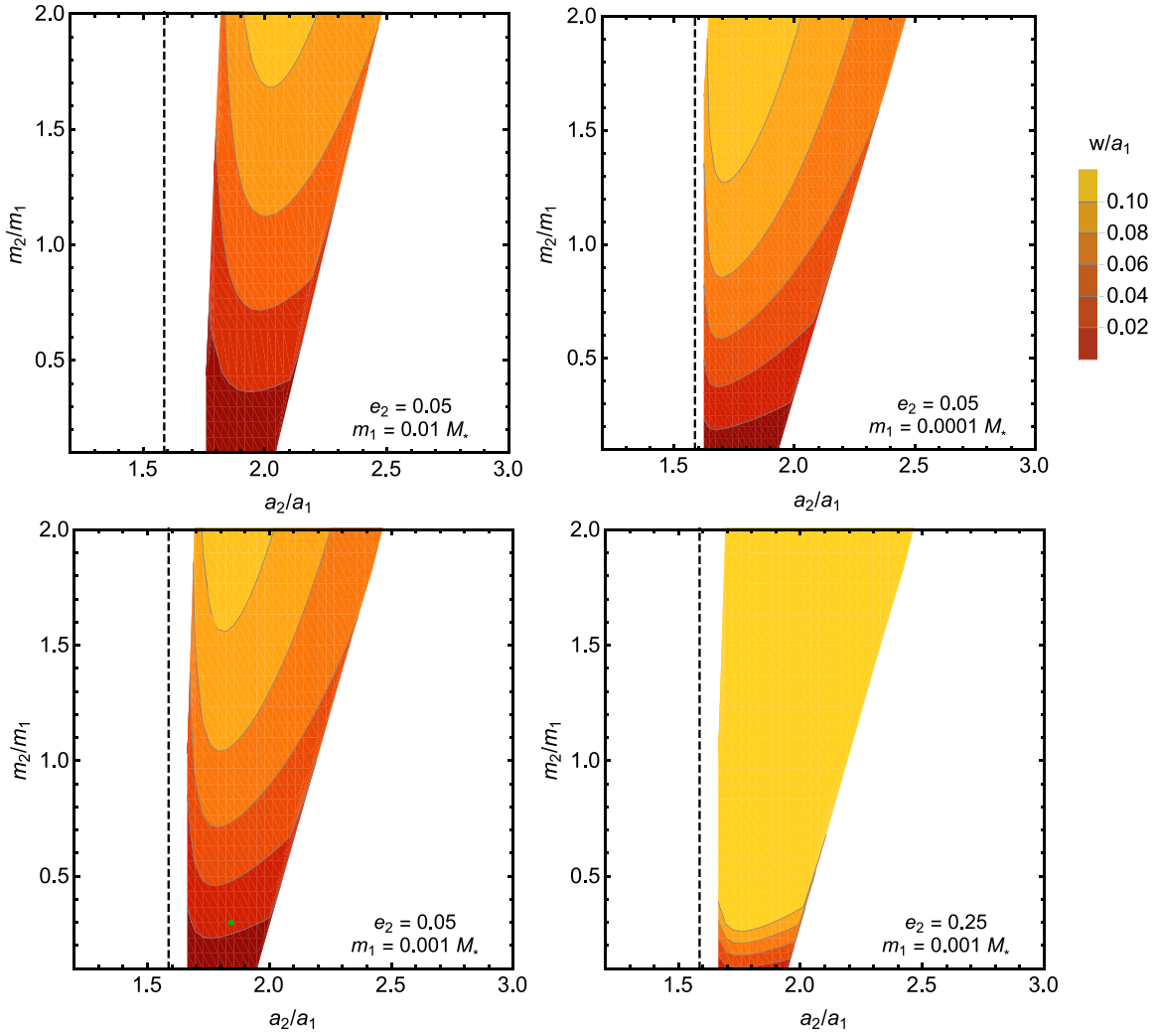


Figure 2. The width of the resonance, w/a_1 , defined to be where $e_f > 0.08$. The inner planet has a mass of $m_1 = 0.01 M_*$ (top left), $m_1 = 0.001 M_*$ (bottom left), and $m_1 = 0.0001 M_*$ (top right), and the outer planet has eccentricity $e_2 = 0.05$. The bottom right panel shows $m_1 = 0.001 M_*$ and $e_2 = 0.25$. The inner-planet eccentricity is $e_1 = 0.05$ in all cases.

Table 1
Exoplanetary Systems with Two or More Planets with Mass Greater than $0.1 M_J$ and Semimajor Axis Greater than 2 au

Host Star	M_*/M_\odot	N_p	P1	P2	a_1/au	a_2/au	m_1/M_J	m_2/M_J	a_{ν_6}/a_1	e_1	e_2	w/a_1
Sun	1.00	8	J	S	5.20	9.58	1.00	0.30	0.37	0.049	0.052	0.025
HD 34445 ^a	1.07	6	b	g	2.07	6.36	0.82	0.38	0.10			
HD 141399	1.07	4	d	e	2.09	5.00	1.18	0.66	0.20			
47 Uma	1.06	3	b	c	2.10	3.60	2.53	0.54	0.53	0.032	0.098	0.021
OGLE-2006-BLG-109L	0.51	2	b	c	2.30	4.50	0.73	0.27	0.32	...	0.15	0.066
UZ For	0.70	2	c	b	2.80	5.90	7.70	6.30	0.33	0.05	0.04	0.037
NN Ser ^a	0.54	2	d	c	3.43	5.35	2.30	7.33	0.92			
HD 66428 ^a	1.05	2	b	c	3.47	23.0	3.20	27.0	0.094			
HU Aqr AB	0.88	2	b	c	3.60	5.40	6.00	4.00	0.80			
HD 30177	0.99	2	b	c	3.70	9.89	8.62	7.60	0.17			
HD 50499	1.31	2	b	c	3.83	9.02	1.64	2.93	0.30	0.266	0.0	0.10
OGLE-2012-BLG-0026L ^a	1.06	2	b	c	4.00	4.80	0.15	0.86	0.90			
HR 8799	1.61	4	e	d	16.4	24.0	10.0	10.0	0.77			
PDS 70	0.76	2	b	c	20.0	34.0	3.00	2.00	0.65			

Notes. Columns (1) and (2) show the name and mass of the host star, respectively. Column (3) shows the number of detected planets in the system. Columns (4)–(9) show the names, semimajor axes, and masses of the giant planets. Column (10) shows the location of the ν_6 resonance. If the resonance is within the belt, the location is shown in bold, and then in Columns (11), (12), and (13) we show the planet eccentricities and the width of the resonance. Where the eccentricity is unknown, we take $e_1 = 0.05$ to calculate the width. The width is where the forced eccentricity $e_f > 0.08$, except for HD 50499, where we take $e_f > 0.3$.

^a System is out of the range of Figure 1.

Table 2
Outcomes of the n -body Simulations

Simulation	a_J/au	a_S/au	N_{Sun}	N_{Earth}	$N_{J,S}$	N_{eject}	N_{outcome}	N_{remain}	P_{collide}
run1	5.2	9.58	288	126	9	1398	1821	8179	0.07
run2	5.2	8.25	1033	30	10	6154	7227	2773	0.004
run3	5.2	...	54	14	12	1050	1130	8870	0.01

Note. Column (1) is the name of the simulation. Columns (2) and (3) are the orbital radii of Jupiter and Saturn, respectively. Columns (4), (5), and (6) show the number of asteroids that hit the Sun, Earth, Jupiter, and Saturn. Column (7) shows the number of asteroids that have been ejected. Column (8) shows the total number of asteroids that have an outcome (either collision or ejection). Column (9) shows the number of asteroids remaining in the simulation. Column (10) shows the probability of an Earth collision for all of the asteroids that have an outcome, $P_{\text{collide}} = N_{\text{Earth}}/N_{\text{outcome}}$.

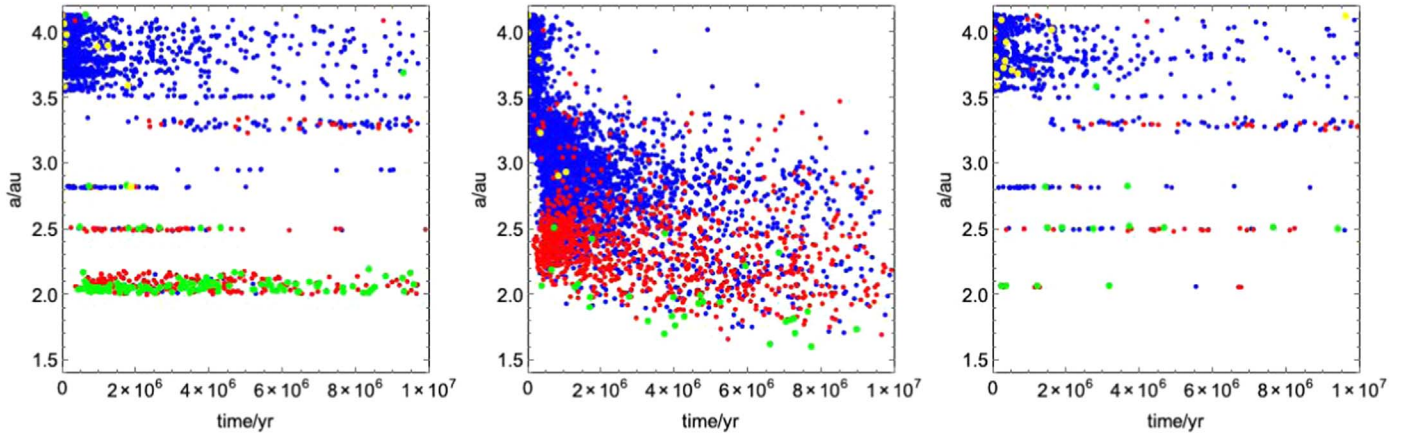


Figure 3. Asteroid outcomes as a function of time and their original semimajor axis, a , for run1 (left), run2 (middle), and run3 (right). Blue points show asteroids that are ejected. Red points show asteroids that collide with the Sun, green points show asteroids that collide with Earth, and yellow points show asteroids that collide with Jupiter or Saturn.

a secular resonance would fall in an asteroid belt (if it exists). This suggests that the particular requirement to have a secular resonance falling within the asteroid belt region does not in itself imply a very stringent fine-tuning on exoplanetary systems for them to allow the emergence of life.

4. Simulations of Asteroid Impacts

We have shown how the architecture of the outer giants affects the location and strength of the ν_6 resonance. However, we have not yet considered how the delivery of asteroids to Earth is affected by the giant planets being close to the 2:1 MMR. We used the n -body code MERCURY (Chambers 1999) with the Blaïre–Stoer integrator to model a belt of 10,000 asteroids in the presence of varying planetary systems. The asteroid belt was initially the same in all simulations. The particles were distributed uniformly in semimajor axis from $a = 1.5$ au out to 4.1 au. The eccentricity was uniformly distributed in the range 0–0.1 and the inclination in the range 0° – 10° . The longitude of ascending node, argument of perihelion, and mean anomaly were all distributed uniformly in the range 0° – 360° . We do not expect the results to change qualitatively for a less dynamically excited belt (e.g., Morbidelli 1993).

Each simulation had Earth at its current location, and we considered three different giant planetary systems as described in Table 2. Run1 describes the current solar system, run2 had the giant planets close to the 2:1 MMR, and run3 had no Saturn. In all of the simulations the size of Earth was inflated to $R_{\text{Earth}} = 10 R_{\oplus}$ in order to artificially increase the number of collisions with Earth. We would expect few to no collisions with Earth in the simulation if Earth was to be taken with its

actual size (see, e.g., Smallwood et al. 2018a). The inflated Earth increases the number of collisions by a factor of 10–100 depending on the relative velocity between Earth and the asteroid, which varies with semimajor axis of the asteroid. In Martin & Livio (2021) we found numerically the range to be approximately 20–30.

Figure 3 shows the outcomes of the simulations as a function of time and the original location of the asteroid. Asteroids are ejected from the system when their semimajor axis becomes larger than 20 au. In Table 2 we tabulate the outcomes of each simulation and calculate the probability of a collision with Earth. Figure 3 shows the initial semimajor axis of asteroids that have an outcome (ejection or collision) and the time of the outcome. The left panel has Jupiter and Saturn at their current locations (run1). Since the asteroids were originally distributed uniformly in semimajor axis, areas of this figure that are white (empty) throughout the simulation still have stable asteroids remaining at the end of the simulation. We therefore find that with Jupiter and Saturn at their current locations, there are large regions of the asteroid belt that remain stable, while some specific resonance locations are cleared out. The outer parts of the belt lie in the chaotic region close to Jupiter, in which there are overlapping MMRs that cause the belt to be unstable. This configuration satisfies the two conditions described in the Introduction. The large empty areas in this figure show that there is still a significant belt that is able to store asteroids in stable configurations (these stable asteroid orbits do not change significantly during the simulation). The ν_6 resonance provides a high collision probability with Earth (Ito & Malhotra 2006; Martin & Livio 2021). The probability of an Earth collision over the entire simulated belt is 0.07. Of course, this is

artificially high because of the inflated size of Earth. Asteroids from stable regions of the belt may be slowly moved into the ν_6 resonance through effects such as asteroid–asteroid interactions, gas drag, the Yarkovsky effect (Farinella et al. 1998), or implantation from farther out (Jewitt et al. 2014; Raymond & Izidoro 2017a).

The right panel of Figure 3 shows the simulation without Saturn (run3). In this case, the inner parts of the asteroid belt are much stabler than when Saturn is included (as in run1) since there is no ν_6 resonance. There are very few collisions or ejections in the inner belt. The few outcomes that occur are a result of MMRs with Jupiter. This configuration satisfies the first criterion in the Introduction—there is a stable asteroid belt. However, there is no efficient mechanism of delivering the asteroids to Earth. The probability of an Earth collision in run3 is 7 times lower than in the simulation with Saturn at its current location (run1). Note that Smallwood et al. (2018a) considered impact rates with a varying location for Saturn. Provided that the ν_6 resonance fell within the belt, the rate of impacts remained high.

The middle panel of Figure 3 shows the outcomes in the simulation in which the giant planets are in resonance (run2). The giant planets display chaotic but stable behavior (see also Izidoro et al. 2016). This leads to stochastic jumps of the secular resonances and a rapid excitation of the asteroid orbits. This simulation, in contrast to the other simulations, shows that most of the asteroid belt is unstable. The resonance between the giant planets leaves stable asteroids only inside of about 1.6 au. The timescale for the ejection of the asteroids is very short. Thus, there is no stable belt in a system with the giant planets in resonance, and we do not satisfy the first criterion described in the Introduction. Despite the unstable belt, there are very few asteroid collisions with Earth. In fact, the probability of an Earth collision is smaller in this case by a factor of 2.5 compared to run3 and by a factor of 18 compared to run1.

5. Discussion and Conclusions

Assuming that asteroid impacts are indeed necessary for the emergence of life, we suggest that there are two requirements on an asteroid belt for a habitable exoplanet to actually be inhabited. First, the exoplanetary system must have the equivalent of an asteroid belt, which may require a giant planet to form outside of the snow line radius with a low eccentricity. Second, the asteroid belt must have a mechanism to deliver asteroids from stable regions of the belt. MMRs with the inner giant planet may not provide a large enough supply of asteroids, and therefore a secular resonance, such as the ν_6 resonance in the solar system, may have to fall within the asteroid belt region. This suggests that a second giant planet is required, its location must fall within a relatively narrow radial region in order for sufficient asteroids to collide with the habitable planet, and its eccentricity must be low. This requires a certain degree of fine-tuning, and it makes the solar system somewhat special (see also Livio 2020). Still, current observations of pairs of giant exoplanets suggest that this configuration is not uncommon.

It is interesting to examine two exoplanetary systems that are high on the list of candidates for the search for life on other exoplanets that are around M dwarfs. TRAPPIST-1 has seven exoplanets, including three Earth-like planets within the habitable zone (Gillon et al. 2016). While there is no evidence for a belt in this system (Marino et al. 2015), we do note that

our own asteroid belt in an exoplanetary system would not be observable (e.g., Wyatt et al. 2007). Comet impacts from a Kuiper Belt equivalent in the system could occur through perturbations from an external perturber (Kral et al. 2018; Raymond et al. 2022). Proxima Centauri has two detected exoplanets, one of which is close to Earth’s size and within the habitable zone (Anglada-Escudé et al. 2016). It is not certain whether an asteroid belt exists in this system (e.g., Siraj & Loeb 2020).

We caution that our conclusions are based on the classical picture of solar system formation. Recently it has been suggested that planetesimals may form in rings that we see in the observations of DSHARP disks (Andrews et al. 2018). Further, it has been suggested that the formation of the planets in the solar system was through rings of planetesimals that formed through pressure bumps (Carrera et al. 2021; Izidoro et al. 2021; Morbidelli et al. 2022). In this picture, asteroid belts lie between the rings, and no giant planet is required for their formation. However, if we require a secular resonance to lie within an asteroid belt, then we still need two giant planets in the system. Furthermore, we do not take into account the migration histories of the giant planets that may deplete the asteroid belt through the motion of the resonances (Minton & Malhotra 2011; Clement et al. 2020).

We thank an anonymous referee for a thorough review and providing useful comments. This research has made use of the NASA Exoplanet Archive, which is operated by the California Institute of Technology, under contract with the National Aeronautics and Space Administration under the Exoplanet Exploration Program (DOI:10.26133/NEA12, NASA Exoplanet Science Institute 2020). Computer support was provided by UNLV’s National Supercomputing Center. R.G.M. acknowledges support from NASA through grant 80NSSC21K0395.

ORCID iDs

Rebecca G. Martin  <https://orcid.org/0000-0003-2401-7168>

References

- Abe, Y., Ohtani, E., Okuchi, T., Righter, K., & Drake, M. 2000, in *Water in the Early Earth*, ed. R. M. Canup et al. (Tucson, AZ: Univ. Arizona Press), 413
- Andrews, S. M., Huang, J., Pérez, L. M., et al. 2018, *ApJL*, 869, L41
- Anglada-Escudé, G., Amado, P. J., Barnes, J., et al. 2016, *Natur*, 536, 437
- Ballerine, N. P., Rieke, G. H., Su, K. Y. L., & Gáspár, A. 2017, *ApJ*, 845, 120
- Beer, M. E., King, A. R., Livio, M., & Pringle, J. E. 2004, *MNRAS*, 354, 763
- Benner, S. A., Bell, E. A., Biondi, E., et al. 2020, *ChemSystemsChem*, 1, e1900035
- Bottke, W. F., & Norman, M. D. 2017, *AREPS*, 45, 619
- Bottke, W. F., Rubincam, J., & Burns, J. A. 2000, *Icar*, 145, 301
- Canup, R. M. 2012, *Sci*, 338, 1052
- Carrera, D., Simon, J. B., Li, R., Kretke, K. A., & Klahr, H. 2021, *AJ*, 161, 96
- Chambers, J. E. 1999, *MNRAS*, 304, 793
- Chambers, J. E., & Wetherill, G. W. 2001, *M&PS*, 36, 381
- Clement, M. S., Morbidelli, A., Raymond, S. N., & Kaib, N. A. 2020, *MNRAS*, 492, L56
- Čuk, M., & Stewart, S. T. 2012, *Sci*, 338, 1047
- DeMeo, F. E., & Carry, B. 2014, *Natur*, 505, 629
- Dermott, S. F., & Nicholson, P. D. 1986, *Natur*, 319, 115
- Farinella, P., Vokrouhlický, D., & Hartmann, W. K. 1998, *Icar*, 132, 378
- Fernandes, R. B., Mulders, G. D., Pascucci, I., Mordasini, C., & Emsenhuber, A. 2019, *ApJ*, 874, 81
- Froeschle, C., & Scholl, H. 1986, *A&A*, 166, 326
- Garaud, P., & Lin, D. N. C. 2007, *ApJ*, 654, 606
- Geiler, F., & Krivov, A. V. 2017, *MNRAS*, 468, 959
- Genda, H., Brasser, R., & Mojszsis, S. J. 2017a, *E&PSL*, 480, 25

- Genda, H., Iizuka, T., Sasaki, T., Ueno, Y., & Ikoma, M. 2017b, *E&PSL*, **470**, 87
- Gillon, M., Jehin, E., Lederer, S. M., et al. 2016, *Natur*, **533**, 221
- Haghighipour, N., & Winter, O. C. 2016, *CeMDA*, **124**, 235
- Hayashi, C. 1981, *PThPS*, **70**, 35
- Ito, T., & Malhotra, R. 2006, *AdSpR*, **38**, 817
- Izidoro, A., Dasgupta, R., Raymond, S. N., et al. 2021, arXiv:2112.15558
- Izidoro, A., Raymond, S. N., Pierens, A., et al. 2016, *ApJ*, **833**, 40
- Jewitt, D., Ishiguro, M., Weaver, H., et al. 2014, *AJ*, **147**, 117
- Kennedy, G. M., & Kenyon, S. J. 2008, *ApJ*, **673**, 502
- Kennedy, G. M., & Wyatt, M. C. 2014, *MNRAS*, **444**, 3164
- Kral, Q., Wyatt, M. C., Triaud, A. H. M. J., et al. 2018, *MNRAS*, **479**, 2649
- Lecar, M., Podolak, M., Sasselov, D., & Chiang, E. 2006, *ApJ*, **640**, 1115
- Livio, M. 2020, in *Fine-tuning in the Physical Universe*, ed. D. Sloan et al. (Cambridge: Cambridge Univ. Press), 412
- Malhotra, R., Fox, K., Murray, C. D., & Nicholson, P. D. 1989, *A&A*, **221**, 348
- Marino, S., Perez, S., & Casassus, S. 2015, *ApJL*, **798**, L44
- Martin, R. G., & Livio, M. 2013a, *MNRAS*, **428**, L11
- Martin, R. G., & Livio, M. 2013b, *MNRAS*, **434**, 633
- Martin, R. G., & Livio, M. 2015, *ApJ*, **810**, 105
- Martin, R. G., & Livio, M. 2021, *MNRAS*, **506**, L6
- Minton, D. A., & Malhotra, R. 2011, *ApJ*, **732**, 53
- Morales, F. Y., Rieke, G. H., Werner, M. W., et al. 2011, *ApJL*, **730**, L29
- Morbidelli, A. 1993, *Icar*, **105**, 48
- Morbidelli, A., Baillié, K., Batygin, K., et al. 2022, *NatAs*, **6**, 72
- Morbidelli, A., Brasser, R., Gomes, R., Levison, H. F., & Tsiganis, K. 2010, *AJ*, **140**, 1391
- Morbidelli, A., Chambers, J., Lunine, J. I., et al. 2000, *M&PS*, **35**, 1309
- Morbidelli, A., Gonzi, R., Froeschle, C., & Farinella, P. 1994, *A&A*, **282**, 955
- Morbidelli, A., & Henrard, J. 1991, *CeMDA*, **51**, 131
- Murray, C. D., & Dermott, S. F. 2000, *Solar System Dynamics* (Cambridge: Cambridge Univ. Press)
- NASA Exoplanet Science Institute 2020, Planetary Systems Table <https://catcopy.ipac.caltech.edu/doi/doi.php?id=10.26133/NEA12PlanetarySystemsTable>, IPAC
- Nesvorný, D., Roig, F. V., & Deienno, R. 2021, *AJ*, **161**, 50
- Nielsen, E. L., De Rosa, R. J., Macintosh, B., et al. 2019, *AJ*, **158**, 13
- O'Brien, D. P., Morbidelli, A., & Bottke, W. F. 2007, *Icar*, **191**, 434
- Osinski, G. R., Cockell, C. S., Pontefract, A., & Sapers, H. M. 2020, *AsBio*, **20**, 1121
- Petit, J.-M., Morbidelli, A., & Chambers, J. 2001, *Icar*, **153**, 338
- Pollack, J. B., Hubickyj, O., Bodenheimer, P., et al. 1996, *Icar*, **124**, 62
- Raymond, S. N., & Izidoro, A. 2017a, *Icar*, **297**, 134
- Raymond, S. N., & Izidoro, A. 2017b, *SciA*, **3**, e1701138
- Raymond, S. N., Izidoro, A., Bolmont, E., et al. 2022, *NatAs*, **6**, 80
- Raymond, S. N., & Nesvorný, D. 2020, arXiv:2012.07932
- Rebollido, I., Eiroa, C., Montesinos, B., et al. 2018, *A&A*, **614**, A3
- Siraj, A., & Loeb, A. 2020, *PSJ*, **1**, 86
- Sleep, N. H. 2018, *AsBio*, **18**, 1199
- Smallwood, J. L., Martin, R. G., Lepp, S., & Livio, M. 2018a, *MNRAS*, **473**, 295
- Smallwood, J. L., Martin, R. G., Livio, M., & Lubow, S. H. 2018b, *MNRAS*, **480**, 57
- Sutherland, J. D. 2016, *AngCh*, **55**, 104
- Sutherland, J. D. 2017, *Nature Reviews Chemistry*, **1**, 1
- Szostak, J. W. 2017a, *AngCh*, **56**, 11037
- Szostak, J. W. 2017b, *Mol. Front. J.*, **1**, 121
- Wetherill, G. W., & Stewart, G. R. 1989, *Icar*, **77**, 330
- Wittenmyer, R. A., Butler, R. P., Tinney, C. G., et al. 2016, *ApJ*, **819**, 28
- Wyatt, M. C., Smith, R., Greaves, J. S., et al. 2007, *ApJ*, **658**, 569
- Zahnle, K. J., Lupu, R., Catling, D. C., & Wogan, N. 2020, *PSJ*, **1**, 11